

## Probability of first return on Cayley trees

This article has been downloaded from IOPscience. Please scroll down to see the full text article.

1997 J. Phys. A: Math. Gen. 30 6995

(<http://iopscience.iop.org/0305-4470/30/20/007>)

View [the table of contents for this issue](#), or go to the [journal homepage](#) for more

Download details:

IP Address: 171.66.16.110

The article was downloaded on 02/06/2010 at 06:03

Please note that [terms and conditions apply](#).

## Probability of first return on Cayley trees

L. Acedo and A. Santos

Departamento de Física, Universidad de Extremadura, E-06071 Badajoz, Spain

Received 11 February 1997, in final form 5 August 1997

**Abstract.** A Lorentz lattice gas with a fraction  $x_B$  of the scatterers being pure backscatterers, the remaining being stochastic (right and left) rotators, is considered. The problem at hand is the evaluation of the probability  $x$  that the moving particle returns to its original site, in the limit where the density  $\rho$  of sites occupied by scatterers is small and the lattice becomes a Cayley tree. In the special case of deterministic collision rules (Gunn–Ortuño model on a Cayley tree), an exact cubic equation for the Laplace transform of the distribution function of first-return times is derived and its asymptotic form near the threshold value  $x_B^c = \frac{2}{3}$  (beyond which  $x = 1$ ) is obtained. In the general case of stochastic models, a mean-field approximation is proposed for  $x$  and the mean return time  $\tau$ . The approximation reduces to the exact result in the case of the deterministic model, as well as in the stochastic model without backscatterers. Comparison with Monte Carlo simulations shows a reasonable agreement in the dependence of  $x$  and  $\tau$  on  $x_B$ . The relevance of the results to the development of approximate analytic expressions for the diffusion coefficient is discussed.

### 1. Introduction

A lot of attention has recently been given to Lorentz lattice gas cellular automata as models to study diffusion phenomena [1]. In these models, a particle moves ballistically in a  $d$ -dimensional regular lattice with a coordination number  $b$ . A fraction  $\rho$  of the sites are occupied by a random quenched array of scatterers. At integer times  $t = 0, 1, 2, \dots$  the particle is located at one of the sites  $r$  of the lattice. If the particle is moving along the direction  $j$  ( $j = 1, 2, \dots, b$ ) and hits a scatterer, it has a probability  $W_{ij}$  of being deflected along the direction  $i$ . To fix ideas, let us consider the rotator model on a square lattice ( $d = 2, b = 4$ ) [2]. In it, a fraction  $x_R$  of the scatterers are stochastic right rotators, a fraction  $x_L$  are stochastic left rotators, and a fraction  $x_B = 1 - x_R - x_L$  are deterministic backscatterers. When the particle collides with a right (left) rotator, it is deflected to the right (left), transmitted, deflected to the left (right), or reflected with probabilities  $\alpha_1, \alpha_2, \alpha_3$ , and  $\beta = 1 - \alpha_1 - \alpha_2 - \alpha_3$ , respectively. If the collision takes place with a pure backscatterer, the particle is reflected with a probability 1. The deterministic case ( $\alpha_1 = 1$ ) was introduced by Gunn and Ortuño [3] and has been analysed by kinetic theory methods and by computer simulations [4–6]. Its main physical motivation is to model the motion of a charged particle in a random magnetic field (e.g. in a turbulent magnetized plasma).

In general, the motion in a Lorentz lattice gas exhibits a diffusive behaviour: the mean-square displacement for long times is of the form  $\langle r^2 \rangle = 2dDt$ , which defines the diffusion coefficient  $D$ ; in addition to it, an important quantity is the probability  $x$  that the particle returns to its initial site for the first time. On the other hand, in the (deterministic) Gunn–Ortuño model with no backscatterers ( $x_B = 0$ ), simulation results by Cohen and Wang [5] show an absence of diffusion due to trapping for all concentrations, except if either  $x_R/x_L$  or

$x_L/x_R$  is equal to a critical value that depends on  $\rho$ ; even in the latter case (where  $D \neq 0$ ), the number of open trajectories decreases with time (as  $t^{-1/7}$ ), so that  $x = 1$ . In this paper, we will be concerned with a special class of Lorentz lattice gases: those on Cayley trees. On a Cayley tree (or Bethe lattice) the particle can return to a site visited before only with velocity opposite to the initial one. On a regular lattice, however, the return can also take place by following a polygonal path or loop. On the other hand, the relevant properties (e.g.  $D$  and  $x$ ) of a  $d$ -dimensional regular lattice with *stochastic* collision rules are identical to those of a Cayley tree in the limit  $d \rightarrow \infty$  as well as in the limit  $\rho \rightarrow 0$  [7, 8]. Such an equivalence does not necessarily hold in the case of deterministic dynamics; once the particle returns to the origin along a closed loop, it will repeat that loop forever.

While a general, direct relationship between  $x$  and  $D$  is not known, such a relationship has been found by van Beijeren and Ernst [7] for Cayley trees with a *single type* of scatterers and by van Beijeren [9] for the Cayley-tree version of the Gunn–Ortuño model. In the case of the rotator model on a Cayley tree with  $x_R = 1$  or  $x_L = 1$ , the exact result is [7]

$$D = \frac{1}{2\rho} \left( \operatorname{Re} \frac{1}{1 - \omega_1} - \frac{x}{1 + x} - \frac{\rho}{2} \frac{1 - x}{1 + x} \right) \quad (1)$$

where  $x < 1$  is obtained from the cubic equation

$$1 = 2 \operatorname{Re} \frac{x + \omega_1}{1 + x\omega_1} + \frac{x - \omega_2}{1 - x\omega_2}. \quad (2)$$

In equations (1) and (2),  $\omega_1 = \alpha_2 - \beta + (\alpha_1 - \alpha_3)i$  and  $\omega_2 = \alpha_2 + \beta - \alpha_1 - \alpha_3$  are eigenvalues of the matrix  $W_{ij}$ . When several types of scatterers are present, the situation is much more complicated, even on a Cayley tree. In the case of the *deterministic* rotator model (Gunn–Ortuño model) on a Cayley tree (with coordination number  $b = 4$ ), however, arguments of percolation theory [10] can be extended to yield a cubic equation for the probability of first return [3]:

$$x = x_B + (1 - x_B)x^3. \quad (3)$$

The meaning of this equation is simple. If the first scatterer found by the particle is a backscatterer (what occurs with probability  $x_B$ ) it returns for sure; if the first scatterer is a rotator (either right or left), the particle must return to that scatterer three successive times along three adjacent directions before it returns to its initial site. The interesting thing is the existence of a threshold value  $x_B^c = \frac{2}{3}$ , such that  $x = 1$  if  $x_B \geq x_B^c$ . Thus, if no more than one out of every three scatterers is a rotator, the particle has a probability 1 of lying on a *finite* cluster (absence of percolation). The exact expression for  $D$  as a function of  $\rho$  and  $x_B$  is [9]:

$$D = \frac{(1 - x)^2}{2\rho} \left( \frac{1}{1 - x(1 - x_B)} - \frac{\rho}{2} \right). \quad (4)$$

Consequently, if  $x_B$  approaches  $x_B^c$  from below,  $D$  goes to zero as  $(x_B^c - x_B)^2$ . Strictly speaking, the quantity  $D$  in equation (4) represents a ‘conductivity’ coefficient, since the collection of particles moving on the lattice falls apart into two subclasses: a fraction  $x^2$  of trapped particles (which do not diffuse) plus a fraction  $1 - x^2$  of mobile particles. The mean-square displacement of the latter defines a ‘true’ diffusion coefficient equal to  $D/(1 - x^2)$ .

The aim of this paper is to analyse some aspects of the Cayley-tree version of the rotator model. First, we consider the *deterministic* case in section 2 and obtain an exact recursion relation for the probability  $P(t)$  that the particle first returns to its initial site after a time  $t$ . By taking into account that  $x = \sum_t P(t)$ , equation (3) is recovered. Also,

the mean return time  $\tau = x^{-1} \sum_t tP(t)$  is obtained exactly. As the backscatterer fraction  $x_B$  approaches the threshold value  $x_B^c = \frac{2}{3}$ ,  $\tau$  diverges as  $|x_B - x_B^c|^{-1}$ . In general,  $P(t)$  verifies a scaling law near the threshold point. A mean-field approximation is worked out in section 3 to obtain estimates of  $x$  and  $\tau$  in the case of the *stochastic* model ( $\alpha_1 < 1$ ). The mean-field character of the approximation is based on the assumption that the probability  $x_n$  that the particle returns  $n$  successive times to any initial site is just  $x_n = x^n$ . Although this assumption is not generally correct, the mean-field approximation reduces to the exact results, equations (2) and (3), in the corresponding limits. In section 4 we compare the mean-field theory predictions with Monte Carlo simulation results for a model without pure backscatterers ( $x_B = 0$ ) and two models including backscatterers ( $x_B > 0$ ). In the first case the agreement is found to be excellent, while it is mainly qualitative in the second class of models. The paper ends with a discussion on the relevance of these results to the development of analytic approximate calculations of the diffusion coefficient in Lorentz lattice gases with a mixture of scatterers.

### 2. Statistics of first-return times in the deterministic model

Let us consider the Gunn–Ortuño model [3] on a Cayley tree. The particle moves on a square lattice where each site is occupied by a scatterer with a probability  $\rho$ . There are three types of scatterers: right rotators (R), left rotators (L), and backscatterers (B), with relative probabilities  $x_R$ ,  $x_L$ , and  $x_B = 1 - x_R - x_L$ , respectively. If the particle arrives at a site occupied by a scatterer, it turns right, turns left, or goes backwards, depending on the type of scatterer found. The motion takes place on a Cayley tree (or Bethe lattice) because the particle recognizes a scatterer visited before only if it moves along a previously explored path. Thus, recollisions along closed loops are ignored. Consequently, the probability  $x$  that the particle first returns to its initial site on the Cayley tree represents the (partial) probability of return by backtracking along previous paths on the regular lattice. As stated in the introduction, this distinction might be relevant, even in the limit  $\rho \rightarrow 0$ .

The probability  $x$  obeys the cubic equation (3). Its physical solution is

$$x = \begin{cases} \frac{1}{2} \left[ \sqrt{1 + 4x_B(1 - x_B)^{-1}} - 1 \right] & x_B < \frac{2}{3} \\ 1 & x_B \geq \frac{2}{3}. \end{cases} \tag{5}$$

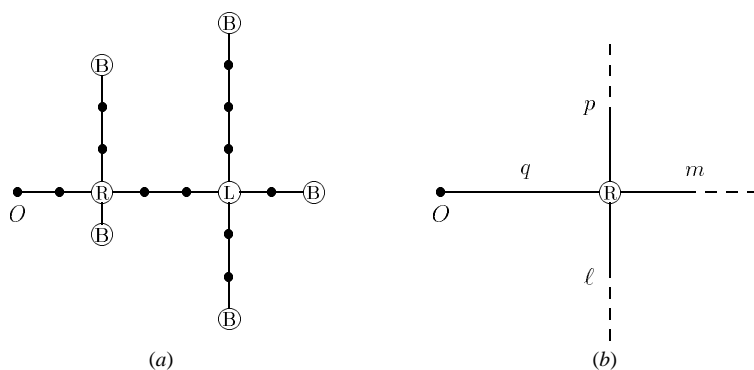


**Figure 1.** (a) A typical trajectory in the Gunn–Ortuño model with a return time  $t = 36$ ; (b) a general returning trajectory.

Our objective in this section is to obtain the distribution of first-return times  $P(t)$ . Figure 1(a) shows a typical trajectory with a return time  $t = 36$ ; in it, the particle visits 18 different sites before returning to the original site ( $O$ ). In general,  $t = 2n$ , where  $n$  is the number of different sites visited. Thus, we can write  $P(t = 2n) \equiv P_n$ . Up to  $n = 3$ , the only scatterer found is a backscatterer:

$$P_n = x_B \rho (1 - \rho)^{n-1} \quad n = 1, 2, 3. \quad (6)$$

For  $n \geq 4$ , the *first* scatterer found in the return trajectory is either a backscatterer or a rotator. In the first case, the contribution to  $P_n$  is given by equation (6). In the second case (sketched in figure 1(b)), the particle must return from the three directions that are explored consecutively. Consequently,

$$P_n = x_B \rho (1 - \rho)^{n-1} + (1 - x_B) \sum_{q+\ell+m+p=n} \rho (1 - \rho)^{q-1} P_\ell P_m P_p \quad n \geq 4 \quad (7)$$

where  $q, \ell, m, p \geq 1$ . This equation can be recast into the form

$$P_n = (1 - \rho) P_{n-1} + \rho (1 - x_B) \sum_{m=2}^{n-2} \sum_{\ell=1}^{m-1} P_{n-1-m} P_{m-\ell} P_\ell \quad n \geq 4 \quad (8)$$

that can be solved recursively. If we introduce the generating function

$$G(z) = \sum_{n=1}^{\infty} e^{-zn} P_n \quad (9)$$

equation (8) becomes

$$[\rho^{-1}(e^z - 1) + 1]G(z) = x_B + (1 - x_B)[G(z)]^3. \quad (10)$$

Obviously, the total probability of first return is

$$x = \sum_{n=1}^{\infty} P_n = G(0) \quad (11)$$

so that equation (3) easily follows from equation (10). Let us define the (normalized) moments

$$\mu_n = \frac{1}{x} \sum_{k=1}^{\infty} k^n P_k = \frac{1}{x} \left( -\frac{d}{dz} \right)^n G(z) \Big|_{z=0}. \quad (12)$$

The recursion relation for the moments is then

$$\mu_n = -\rho^{-1} \sum_{m=0}^{n-1} (-1)^{n+m} \binom{n}{m} \mu_m + (1 - x_B) x^2 \sum_{m=0}^n \sum_{\ell=0}^{n-m} \binom{n}{m} \binom{n-m}{\ell} \mu_m \mu_\ell \mu_{n-m-\ell}. \quad (13)$$

In particular, the mean return time (of those particles that do return) is

$$\tau \equiv 2\mu_1 = \frac{2\rho^{-1}}{1 - 3x^2(1 - x_B)} \quad (14)$$

and the variance is

$$\sigma^2 \equiv 4(\mu_2 - \mu_1^2) = 4\rho^{-2} \frac{1 - \rho + 3x^2(1 - x_B)[1 + 2\rho - 3\rho x^2(1 - x_B)]}{[1 - 3x^2(1 - x_B)]^3}. \quad (15)$$

Proceeding in a similar way, one can obtain any moment as a function of  $\rho$  and  $x_B$ . The probability  $P_n$  can be obtained from equation (8) or, equivalently, by solving the cubic equation (10) and using the relation

$$P_n = \frac{1}{n!} \left( -e^z \frac{d}{dz} \right)^n G(z) \Big|_{z \rightarrow \infty}. \quad (16)$$

As  $x_B$  approaches the threshold value  $x_B = \frac{2}{3}$ ,  $\tau$  diverges as  $|x_B - \frac{2}{3}|^{-1}$ . In general,  $\mu_n \sim |x_B - \frac{2}{3}|^{-(2n-1)}$ ,  $n \geq 1$ . These results can be reinterpreted from the point of view of percolation theory [10]. Thus,  $x$  is the probability that the origin (or any other arbitrary selected site) belongs to a *finite* cluster,  $1 + 4\mu_1$  is the average number of sites of the finite clusters, and  $x^{-1}P_n$  is the probability that a finite cluster has  $1 + 4n$  sites. Only if  $x_B < \frac{2}{3}$  is there percolation (the particle may not return). Near the percolation threshold the sizes of the finite clusters become very large.

In the limit  $\rho \rightarrow 0$ , time becomes a continuous variable, and  $P(t)$  becomes a probability density. We define

$$t^* = \rho t \quad \Delta t^* = 2\rho \quad f(t^*) = \frac{1}{\Delta t^*} P(t). \tag{17}$$

Thus, in the limit  $\rho \rightarrow 0$ , equation (8) yields the integro-differential equation

$$f'(t^*) = -\frac{1}{2}f(t^*) + \frac{1}{2}(1 - x_B) \int_0^{t^*} dt_1^* \int_0^{t_1^*} dt_2^* f(t^* - t_1^*)f(t_1^* - t_2^*)f(t_2^*) \tag{18}$$

with the initial condition  $f(0) = \frac{1}{2}x_B$ . The Laplace transform

$$F(s) = \int_0^\infty dt^* e^{-st^*} f(t^*) \tag{19}$$

obeys the cubic equation

$$(2s + 1)F(s) = x_B + (1 - x_B)[F(s)]^3. \tag{20}$$

This equation can also be obtained from equation (10) by making the changes  $s = z/2\rho$ ,  $F(s) = G(z)$ , and taking the limit  $\rho \rightarrow 0$ .

Although  $F(s)$  can be explicitly obtained, it does not allow us to obtain an explicit expression for  $f(t^*)$ . On the other hand, a useful approximation for long times and near the threshold can be easily obtained. In the limit  $x_B \rightarrow \frac{2}{3}$ ,  $\tau^* \equiv \rho\tau$  diverges as  $\tau^* \approx \frac{2}{3}|x_B - \frac{2}{3}|^{-1}$ . Thus, at  $x_B = \frac{2}{3}$ ,  $f(t^*) = f_c(t^*)$  must exhibit an algebraic tail and  $F(s) = F_c(s)$  must be singular at  $s = 0$ . In fact,  $s = 0$  is a branch point and  $F_c(s) = 1 - (2s)^{1/2} + \mathcal{O}(s)$ . For small  $s$ , this is consistent with

$$F_c(s) \approx e^{-\sqrt{2s}}. \tag{21}$$

Its inverse Laplace transform [11] is the Smirnov density [12]

$$f_c(t^*) \approx \frac{1}{\sqrt{2\pi}} t^{*-3/2} e^{-1/2t^*}. \tag{22}$$

Of course, there exists an infinite number of approximations consistent with the correct asymptotic behaviour  $f_c(t^*) \sim t^{*-3/2}$ . The main reason to choose equations (21) and (22) is that they offer an excellent compromise between simplicity and accuracy. For instance, one could have taken  $F_c(s) \approx (1 + \sqrt{2s})^{-1}$ , which yields  $f_c(t^*) \approx (2\pi t^*)^{-1/2} - \frac{1}{2}e^{t^*/2} \operatorname{erfc}\sqrt{t^*}/2$ . Comparison with the exact  $f_c(t^*)$  obtained numerically shows that the latter approximation has a relative error at least four times larger than that of equation (22) for  $t^* > 10$ .

Let us consider now the case  $x_B \neq \frac{2}{3}$ . In the limit  $s \rightarrow 0$  the solution to equation (20) is

$$F(s) = x[1 - \tau^*s + \frac{1}{2}\tau^{*3}s^2 + \mathcal{O}(s^3)]. \tag{23}$$

A consistent approximation that reduces to equation (21) is

$$F(s) \approx x e^{a(\sqrt{s_0} - \sqrt{s+s_0})} \tag{24}$$

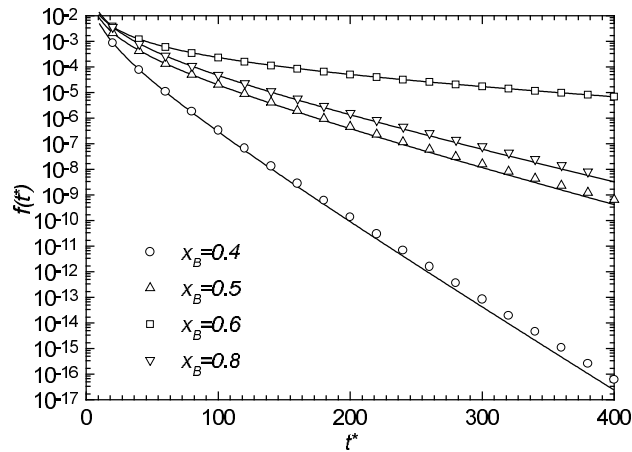


**Figure 2.** Distribution of first-return times in the Gunn–Ortuño model for  $x_B = 0.4, 0.5, 0.6, 0.8$ . The lines correspond to the asymptotic expression (26) and the symbols correspond to the exact values obtained at the density  $\rho = 0.1$ .

where

$$s_0 = [2\tau^*(\tau^* - 1)]^{-1} \quad a = 2\tau^*\sqrt{s_0}. \quad (25)$$

The function (24) has a branch point ( $s = -s_0$ ) different from the actual one  $s = -s'_0 = -\frac{1}{2}[1 - (\frac{3}{2}x_B)^{\frac{2}{3}}(3 - 3x_B)^{1/3}]$ . However,  $s_0 \approx s'_0 \approx \frac{9}{8}(x_B - \frac{2}{3})^2$  near the threshold. The inverse Laplace transform of (24) [11] gives the long-time behaviour of  $f(t^*)$ :

$$f^*(t^*) \approx x \frac{a}{2\sqrt{\pi}} e^{a\sqrt{s_0}t^* - 3/2} e^{-s_0 t^* - a^2/4t^*}. \quad (26)$$

In figure 2 we have compared the asymptotic distribution (26) for  $x_B = 0.4, 0.5, 0.6$  and  $0.8$  with the *exact* one obtained from equation (8) at the *finite* density  $\rho = 0.1$ . The good agreement observed in figure 2 shows the reliability of equation (26), even outside the regime of long times and small values of  $|x_B - \frac{2}{3}|$  and  $\rho$ .

### 3. Probability of first return in stochastic models

In this section we consider the stochastic version of the original Gunn–Ortuño model. The backscatterers still reverse the direction of motion of the particle. On the other hand, if the particle hits a right rotator, it is deflected to the right with probability  $\alpha_1$ , transmitted with probability  $\alpha_2$ , deflected to the left with probability  $\alpha_3$ , or reflected with probability  $\beta = 1 - \alpha_1 - \alpha_2 - \alpha_3$ ; collision with a left rotator proceeds in an equivalent way. If we particularize to  $\alpha_1 = 1$  we recover the deterministic model of the preceding section. The calculation of the probability of first return is now much more complicated since many more trajectories need to be enumerated.

Our aim here is to obtain an *approximate* closed equation for  $x$ . The basic approximation consists of assuming that  $x_n = x^n$ , where  $x_n$  denotes the probability that the particle returns  $n$  successive times to the origin. From that point of view, the method can be interpreted as a *mean-field* approximation. That  $x_n \neq x^n$  can be easily seen in the deterministic model. In that case, if the origin is not occupied by a scatterer, then  $x_n = x^2$ ,  $n \geq 2$ ; if it is occupied

by a backscatterer, then  $x_n = x$ ,  $n \geq 1$ ; finally, if the origin is occupied by a rotator, then  $x_n = x^4$ ,  $n \geq 4$ . Consequently, the average probability of  $n$  returns is

$$x_n = \rho x_B x + \rho(1 - x_B)x^{a_n} + (1 - \rho)x^{b_n} \quad (27)$$

where  $a_n = n$  if  $n \leq 4$  and  $a_n = 4$  otherwise, and  $b_1 = 1$ ,  $b_n = 2$  if  $n \geq 2$ .

In the stochastic model, equation (3) can be replaced by

$$x = x_B + (1 - x_B)y \quad (28)$$

where  $y$  is the net probability that the particle returns to the origin, provided that the *first* scatterer found was not a backscatterer. Our mean-field approximation consists of writing

$$y(x) = \beta + \gamma_1 x + \gamma_2 x^2 + \gamma_3 x^3 + \dots \quad (29)$$

The term  $\gamma_n x^n$  is the probability that the particle is deflected by the scatterer, returns to it  $n$  times, and then moves to the origin. Obviously,  $\gamma_0 = \beta$ . The probabilities  $\gamma_1$  and  $\gamma_2$  are

$$\gamma_1 = \alpha_1 \alpha_3 + \alpha_2 \alpha_2 + \alpha_3 \alpha_1 \quad (30)$$

$$\gamma_2 = \alpha_1(\beta \alpha_3 + \alpha_1 \alpha_2 + \alpha_2 \alpha_1) + \alpha_2(\beta \alpha_2 + \alpha_1 \alpha_1 + \alpha_3 \alpha_3) + \alpha_3(\beta \alpha_1 + \alpha_3 \alpha_2 + \alpha_2 \alpha_3). \quad (31)$$

In general, we can write

$$\gamma_n = \alpha_1 \gamma_n^{(1)} + \alpha_2 \gamma_n^{(2)} + \alpha_3 \gamma_n^{(3)}. \quad (32)$$

For instance,  $\gamma_n^{(2)}$  is the probability that the particle, having been transmitted by the scatterer first and having returned  $n$  times to it, moves finally to the origin. Thus, the following recursion relations hold

$$\gamma_{n+1}^{(1)} = \beta \gamma_n^{(1)} + \alpha_1 \gamma_n^{(2)} + \alpha_2 \gamma_n^{(3)} \quad (33)$$

$$\gamma_{n+1}^{(2)} = \beta \gamma_n^{(2)} + \alpha_1 \gamma_n^{(3)} + \alpha_3 \gamma_n^{(1)} \quad (34)$$

$$\gamma_{n+1}^{(3)} = \beta \gamma_n^{(3)} + \alpha_3 \gamma_n^{(2)} + \alpha_2 \gamma_n^{(1)} \quad (35)$$

with the initial conditions  $\gamma_1^{(1)} = \alpha_3$ ,  $\gamma_1^{(2)} = \alpha_2$ ,  $\gamma_1^{(3)} = \alpha_1$ . It is worth remarking that, in the special case of  $\alpha_1 = 1$  (Gunn–Ortuño model), one has  $\gamma_n = \delta_{n,3}$  and equation (29) gives the exact result  $y = x^3$ , even though  $x_n \neq x^n$ . In matrix form, equations (33)–(35) are equivalent to

$$\gamma_{n+1} = \mathbf{M} \cdot \gamma_n = \mathbf{M}^n \cdot \gamma_1 \quad (36)$$

where

$$\gamma_n = \begin{pmatrix} \gamma_n^{(1)} \\ \gamma_n^{(2)} \\ \gamma_n^{(3)} \end{pmatrix} \quad \mathbf{M} = \begin{pmatrix} \beta & \alpha_1 & \alpha_2 \\ \alpha_3 & \beta & \alpha_1 \\ \alpha_2 & \alpha_3 & \beta \end{pmatrix}. \quad (37)$$

The eigenvalues of  $\mathbf{M}$  are  $\lambda_i = \beta - \beta_i$  ( $i = 0, \pm$ ), where

$$\beta_0 = -\frac{2}{3}h^{1/2} \cosh \left[ \frac{1}{3} \cosh^{-1} \left( \frac{c}{h^{3/2}} \right) \right] \quad (38)$$

$$\beta_{\pm} = -\frac{1}{2}\beta_0 \pm i \left( \frac{3}{4}\beta_0^2 - \frac{h}{3} \right)^{1/2} \quad (39)$$

with  $c \equiv \frac{27}{2}\alpha_2(\alpha_1^2 + \alpha_3^2)$ ,  $h \equiv 3(\alpha_2^2 + 2\alpha_1\alpha_3)$ . Thus,

$$\mathbf{M} = \mathbf{U} \cdot \mathbf{D} \cdot \mathbf{U}^{-1} \quad (40)$$



where  $\mathbf{D}$  is the diagonal matrix with elements  $\lambda_0$ ,  $\lambda_+$ , and  $\lambda_-$ , and

$$\mathbf{U} = \begin{pmatrix} \alpha_3\alpha_2 - \alpha_1\beta_0 & \alpha_3\alpha_2 - \alpha_1\beta_+ & \alpha_3\alpha_2 - \alpha_1\beta_- \\ \beta_0^2 - \alpha_2^2 & \beta_+^2 - \alpha_2^2 & \beta_-^2 - \alpha_2^2 \\ \alpha_1\alpha_2 - \alpha_3\beta_0 & \alpha_1\alpha_2 - \alpha_3\beta_+ & \alpha_1\alpha_2 - \alpha_3\beta_- \end{pmatrix}. \quad (41)$$

Substitution into equation (36) yields

$$\gamma_n = A_0\lambda_0^{n-1} + A_+\lambda_+^{n-1} + A_-\lambda_-^{n-1} \quad (42)$$

where

$$A_i = \frac{(2\alpha_2^2 + \beta_{i+1}\beta_{i-1})[(\alpha_1^2 + \alpha_3^2)\beta_i + \alpha_2(\alpha_2^2 - \beta_i^2 - 2\alpha_1\alpha_3)]}{\alpha_2(\beta_i - \beta_{i+1})(\beta_{i-1} - \beta_i)} \quad (43)$$

with the convention  $\beta_{i\pm 3} = \beta_i$ . Finally, insertion of equation (42) into equation (29) gives

$$y(x) = \beta + x \left( \frac{A_0}{1 - \lambda_0 x} + \frac{A_+}{1 - \lambda_+ x} + \frac{A_-}{1 - \lambda_- x} \right). \quad (44)$$

Equations (28) and (44) give an (approximate) quartic equation for the probability  $x$  of first return in terms of the fraction of backscatterers  $x_B$  and the scattering probabilities  $\beta$ ,  $\alpha_1$ ,  $\alpha_2$ , and  $\alpha_3$ . It is easy to prove the identities

$$\frac{A_0}{1 - \lambda_0} + \frac{A_+}{1 - \lambda_+} + \frac{A_-}{1 - \lambda_-} = 1 - \beta \quad (45)$$

$$\frac{A_0}{(1 - \lambda_0)^2} + \frac{A_+}{(1 - \lambda_+)^2} + \frac{A_-}{(1 - \lambda_-)^2} = 3. \quad (46)$$

Equation (45) implies that  $x = 1$  is a mathematical solution to equation (28), while equation (46) implies that  $x_B^c = \frac{2}{3}$  is the threshold fraction, beyond which the physical solutions is  $x = 1$ . In the region  $x_B \lesssim \frac{2}{3}$ , one has  $y(x) \approx 1 - 3(1 - x) + B(1 - x)^2$ , where

$$B = A_0 \frac{\lambda_0}{(1 - \lambda_0)^3} + A_+ \frac{\lambda_+}{(1 - \lambda_+)^3} + A_- \frac{\lambda_-}{(1 - \lambda_-)^3}. \quad (47)$$

Equation (28) then gives

$$x \approx 1 - \frac{9}{B} \left( \frac{2}{3} - x_B \right). \quad (48)$$

In the stochastic model with a single type of rotator ( $x_R = 1$  or  $x_L = 1$ ), equations (28) and (44) yield

$$\frac{A_0}{1 - \lambda_0} \frac{1}{1 - \lambda_0 x} + \frac{A_+}{1 - \lambda_+} \frac{1}{1 - \lambda_+ x} + \frac{A_-}{1 - \lambda_-} \frac{1}{1 - \lambda_- x} = 1 \quad (49)$$

where use has been made of equation (45) to eliminate the unphysical root  $x = 1$ . After some algebra, it can be verified that equations (2) and (49) are equivalent cubic equations. Since our mean-field approximation for the probability of first return becomes exact both in the deterministic case for a mixture of scatterers (as stated above equation (36)) and in the stochastic case for single scatterers, one can expect that it gives reasonable estimates in the general case.

Following the same reasoning as in equations (28) and (29), one can obtain an estimate of the reduced mean return time  $\tau^*$ . In the spirit of our mean-field approximation, if the particle leaves the origin, hits a scatterer, returns to it  $n$  times and then goes back to the origin, it has spent an average time equal to  $2 + n\tau^*$ . Consequently,

$$\begin{aligned} x\tau^* &= 2x_B + (1 - x_B)[2\beta + \gamma_1 x(2 + \tau^*) + \gamma_2 x^2(2 + 2\tau^*) + \gamma_3 x^3(2 + 3\tau^*) + \dots] \\ &= 2x + (1 - x_B)x\tau^*y'(x) \end{aligned} \quad (50)$$

where  $y'(x) = dy/dx$  and in the last step we have made use of equation ((29). Thus,

$$\tau^{*-1} = \frac{1}{2}[1 - (1 - x_B)y'(x)]. \quad (51)$$

In the deterministic case,  $y'(x) = 3x^2$  and we recover equation (14). In the stochastic model, one gets the universal behaviour  $\tau^* \approx \frac{2}{3}|x_B - \frac{2}{3}|^{-1}$  in the region  $x \approx \frac{2}{3}$ , which is exact in the deterministic case.

As an example of a pure stochastic model with  $x_B \neq 0$ , let us take  $\alpha_1 = \alpha_2 = \alpha_3 = (1 - \beta)/3$ . Then,  $\beta_0 = -2\alpha_1$ ,  $\beta_{\pm} = \alpha_1$ ,  $A_0 = 3\alpha_1^2$ ,  $A_{\pm} = 0$  and one has

$$x = \begin{cases} 1 - 3\frac{1 - \beta}{2 + \beta} \left( \frac{2}{3} - x_B \right) & x_B < \frac{2}{3} \\ 1 & x_B \geq \frac{2}{3} \end{cases} \quad (52)$$

$$\tau^{*-1} = \begin{cases} \frac{2 - 3x_B}{6(1 - x_B)} & x_B < \frac{2}{3} \\ \frac{3}{2}(x_B - \frac{2}{3}) & x_B \geq \frac{2}{3}. \end{cases} \quad (53)$$

Before closing this section, it is worthwhile remarking that the theoretical prediction  $x_B^c = \frac{2}{3}$  must be correct, even for stochastic models. From a static viewpoint, a non-percolating cluster consists of a collection of bonds with nodal points at the locations of the rotators, bounded in all directions by pure backscatterers. The precise nature of the rotators is unimportant, as long as they allow a returning particle to explore all directions from the nodal point. Thus, a trivial exception is the (one-dimensional) model with  $\alpha_1 = \alpha_3 = 0$ , in which case  $x = 1$  for all  $x_B$ , i.e.  $x_B^c = 0$ .

#### 4. Monte Carlo simulations

In order to test the mean-field theory results obtained in the previous section, we have performed Monte Carlo simulations for some of the models. In an arbitrary realization of the system (with  $\rho \rightarrow 0$ ) we have followed the motion of  $N$  particles over a finite period of time  $t_0^*$ . The fraction of particles returning to the origin gives  $x$ , while the mean return time of those particles gives  $\tau^*$ . Since  $t_0^*$  is finite, we actually get lower bounds of  $x$  and  $\tau^*$ ; those particles that might return after a time  $t^* > t_0^*$  are not accounted for. This is especially important near the threshold, where the distribution of return times is expected to have an algebraic tail (see equation (22) for the deterministic model) and the mean return time is expected to diverge. In the simulations, we have typically taken  $N = 10^6$  and  $t_0^* = 10^3$ , save for the percolation region.

We consider first a stochastic rotator model with  $\alpha_1 = 1 - 2\beta$ ,  $\alpha_2 = \beta$ ,  $\alpha_3 = 0$  in the absence of backscatterers ( $x_B = 0$ ). In figures 3 and 4 the simulation results are compared with the mean-field theory predictions, equations (28), (44), and (51). The agreement is found to be excellent. It is important to notice that the analytical predictions are independent of the relative fraction of right and left rotators and coincide with that of single scatterer models, equation (49). Reasons explaining this agreement between Monte Carlo simulations and the mean-field theory approximation will be discussed in the last section.

The most physically interesting models are those including backscatterers. We have considered the isotropic model ( $\alpha_1 = \alpha_2 = \alpha_3 = \beta = \frac{1}{4}$ ) and the model with  $\alpha_1 = \alpha_2 = \alpha_3 = \frac{1}{3}$ ,  $\beta = 0$ . The mean-field predictions are given by equations (52) and (53). Figures 5 and 6 show  $x$  and  $\tau^*$ , respectively, as functions of  $x_B$ . In the region  $0.50 < x_B < 0.72$ , we have taken  $N = 10^7$  and  $t_0^* = 1.5 \times 10^3$ . We observe in figure 5 that, although the dependence of  $x$  on  $x_B$  is not strictly linear in the simulation results, the

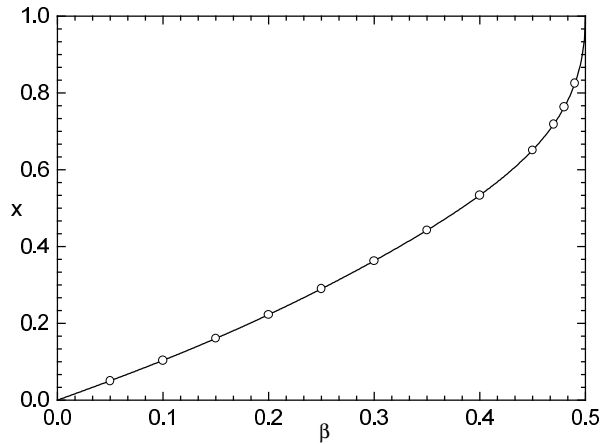


**Figure 3.** First-return probability for the rotator model with  $\alpha_1 = 1 - 2\beta$ ,  $\alpha_2 = \beta$ ,  $\alpha_3 = 0$  in the absence of backscatterers. The Monte Carlo data are denoted by circles. The full curve is the mean-field theory prediction.

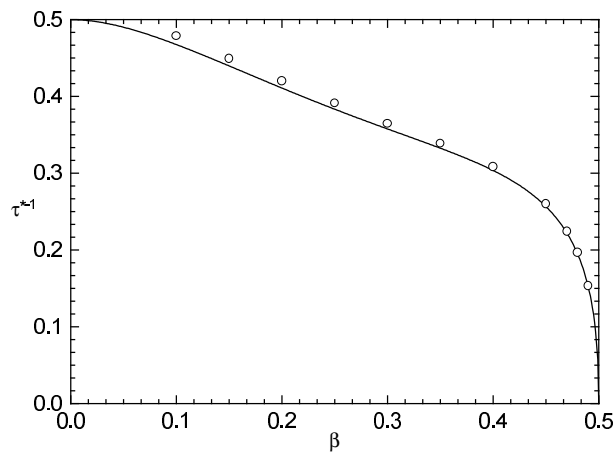


**Figure 4.** The same as figure 3, but for the inverse mean return time.

mean-field theory gives reasonable estimates, the deviations being smaller than 5%. Also, the threshold value beyond which all particles return (and the diffusion coefficient vanishes [13]) is consistent with the theoretical prediction  $x_B^c = \frac{2}{3}$ . On the other hand, the way  $x \rightarrow 1$  as  $x_B \rightarrow x_B^c$  is smoother than that predicted by the theory, thus indicating a critical exponent larger than 1. The discrepancies between simulation results and mean-field theory predictions are more important in the case of the mean return time  $\tau^*$ , as shown in figure 6. The agreement is good near  $x_B = 0$  or  $x_B = 1$ , but worsens at intermediate concentrations of backscatterers. At a qualitative level, it is remarkable that the results with  $\beta = \frac{1}{4}$  and  $\beta = 0$  are practically indistinguishable, in agreement with the theory. Apparently, the mean return time in the simulations does not diverge for any value of  $x_B$ . The maximum value of  $\tau^*$  in the case of isotropic scatterers, for instance, is  $\tau_{\max}^* \simeq 18$ . This is obviously an artifact due to the unavoidable use of finite values of  $N$  and  $t_0^*$  in the simulations. To explore this effect, we have also considered  $N = 10^8$  and  $t_0^* = 10^4$  for the isotropic model and the results

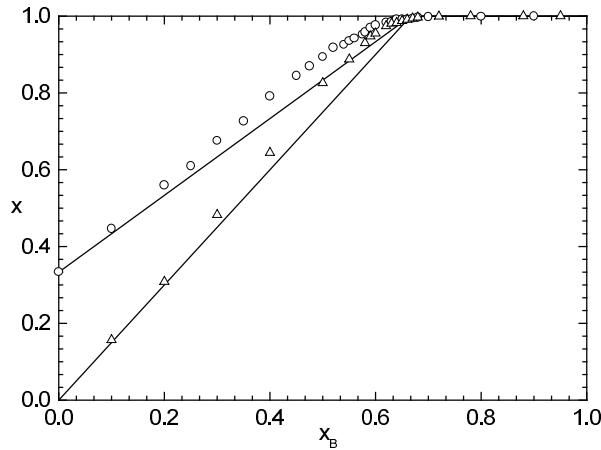


**Figure 5.** First-return probability as a function of the fraction  $x_B$  of backscatterers for the stochastic model with  $\alpha_1 = \alpha_2 = \alpha_3 = (1 - \beta)/3$  in the case of isotropic scatterers ( $\beta = \frac{1}{4}$ , circles) and scatterers without reflection ( $\beta = 0$ , triangles). The symbols refer to Monte Carlo results and the full lines correspond to the mean-field theory predictions.

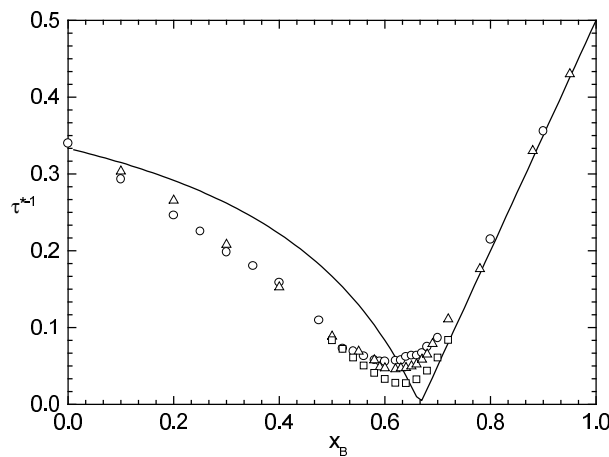


**Figure 6.** The same as figure 5, but for the inverse mean return time. The squares are Monte Carlo data for the isotropic model obtained with  $N = 10^8$  and  $t_0^* = 10^4$ .

are represented by squares in figure 6. Now the maximum value is  $\tau_{\max}^* \simeq 36$ . From the location of  $\tau_{\max}^*$  one can get an *apparent* threshold fraction  $x_B^c \simeq 0.62$ . This is supported by figure 7, which shows a log-log plot of the distribution of first-return times in the isotropic model at  $x_B = 0.62$ , as obtained from the Monte Carlo simulations with  $N = 10^8$  and  $t_0^* = 10^4$ . A linear fit suggests a (normalized) distribution  $f_c(t^*) \approx 0.4336t^{*-1.62}e^{-0.47/t^*}$ . This distribution is analogous to that of the deterministic case, equation (22), except that now the Fisher exponent [10] is 2.62 instead of  $\frac{5}{2}$ . If one defines an *apparent* mean return time  $\tau_{\max}^*(t_0^*) = \int_0^{t_0^*} dt^* t^* f_c(t^*)$ , one gets values consistent with the simulation results.

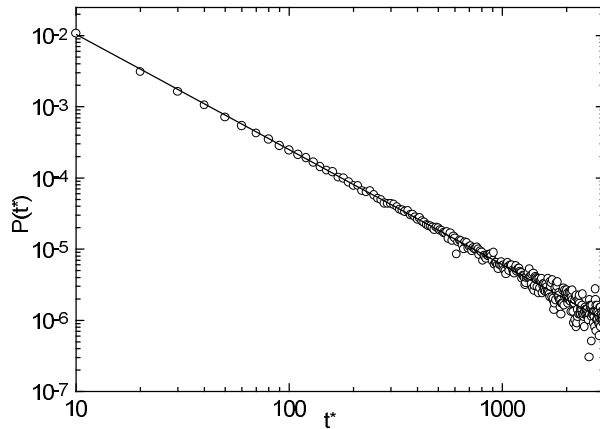


**Figure 7.** Distribution of first-return times for a model of isotropic scatterers with a fraction  $x_B = 0.62$  of backscatterers. The circles denote Monte Carlo data and the full line is a linear fit.

## 5. Discussion

In this paper we have been dealing with the probability of first return on Lorentz lattice gases (in the Cayley-tree limit) where the scatterers are stochastic rotators and deterministic backscatterers. In the special case of deterministic rotators (Gunn–Ortuño model), an exact analytic equation in the Laplace space has been derived for the distribution of return times. As the fraction  $x_B$  of backscatterers approaches the threshold value  $x_B^c = \frac{2}{3}$  from below, the probability of first return  $x$  goes to 1 and the mean return time  $\tau$  diverges; for  $x_B > x_B^c$ ,  $x = 1$ . The long-time behaviour near the threshold has been derived and compared favorably with an exact evaluation at finite density.

In section 3 we have developed a mean-field theory for  $x$  and  $\tau$  by assuming that the successive probabilities of return to a given site along a given path are statistically independent; this is equivalent to the assumption that the scatterers are newly placed on the lattice, according to their relative fractions, every time the particle explores a path. Although not correct in general, the above ansatz is valid for the single scatterer model (because  $x$  is then independent of the configuration of scatterers) and for the deterministic model (because the paths are visited only once before returning to the origin). The mean-field theory assumption is also correct for models with two types of scatterers with a symmetrical set of deflecting probabilities (left and right rotators without backscatterers), since the return probability to a given site is again independent of the configuration of scatterers. This is confirmed by comparison with Monte Carlo simulations. If backscatterers are introduced in the model ( $x_B \neq 0$ ), the symmetry is broken and the agreement with Monte Carlo simulation data is only qualitative, but reasonable. The mean-field theory predicts the existence of a threshold  $x_B^c = \frac{2}{3}$ , even for stochastic models, so that  $x \rightarrow 1$  and  $\tau \rightarrow \infty$  as  $x_B \rightarrow x_B^c$ . This agrees with the Monte Carlo simulations.

This mean-field theory could be improved by including the effect of the next-nearest neighbours of the first scatterer visited and then making an average over all configurations of these scatterers. Preliminary results show a much better agreement with simulations than that of the first-order mean-field theory discussed in this paper, especially outside the percolation region. Possible renormalization of this theory by using the self-similarity of the Cayley tree is also worth studying.

To conclude, let us comment on the possible interest of the results reported in this paper to the evaluation of the diffusion coefficient  $D$  in Lorentz lattice gases with a mixture of *stochastic* scatterers. In the case of single scatterer models,  $D$  is related to the total return probability  $x$  by means of equation (1) and  $x$  obeys the cubic equation (2), both of them being exact [7]. In the case of mixtures, approximate expressions similar to equations (1) and (2) have been obtained by computing the effect of repeated ring (RR) collisions in a self-consistent way [2]. This approximation is in excellent agreement with Monte Carlo simulations in the absence of backscatterers [14], but predicts a diffusive percolation threshold  $x_B^c = \frac{1}{3}$  that is in contrast with simulation results, which indicate a much larger threshold compatible with  $x_B^c = \frac{2}{3}$  [13, 14]. A better approximation can be developed if one retains the relationship between  $D$  and  $x$  provided by the RR approximation, but uses the algebraic equation for  $x$  obtained in this paper or the improved one mentioned above. Work along this line is currently in progress and will be published elsewhere.

### Acknowledgments

We are grateful to Santos Bravo Yuste for his helpful comments and a critical reading of the manuscript. Partial support from the DGICYT (Spain) through grant no PB94-1021 and from the Junta de Extremadura-Fondo Social Europeo through grant no EIA94-39 is acknowledged. The research of LA has been supported by the Ministerio de Educación y Ciencia (Spain).

### References

- [1] Ernst M H 1991 *Liquids, Freezing and Glass Transitions* ed J P Hansen, D Levesque and J Zinn-Justin (Amsterdam: Elsevier) pp 43–143
- [2] Ossendrijver A J H, Santos A and Ernst M H 1993 *J. Stat. Phys.* **71** 1015
- [3] Gunn J M F and Ortuño M 1985 *J. Phys. A: Math. Gen.* **18** L1035
- [4] Kong X P and Cohen E G D 1991 *Physica* **47D** 9
- [5] Cohen E G D and Wang F 1995 *J. Stat. Phys.* **81** 445
- [6] van Velzen G A 1991 *J. Phys. A: Math. Gen.* **24** 787
- [7] van Beijeren H and Ernst M H 1993 *J. Stat. Phys.* **70** 793
- [8] Ernst M H, van Velzen G A and Binder P M 1989 *Phys. Rev. A* **39** 4327
- [9] van Beijeren H unpublished
- [10] Stauffer D and Aharony A 1994 *Introduction to Percolation Theory* (London: Taylor and Francis)
- [11] Spiegel M R 1967 *Laplace Transforms* (New York: McGraw-Hill)
- [12] Hughes H D 1995 *Random Walks and Random Environments. Volume 1: Random Walks* (Oxford: Clarendon)
- [13] Acedo L and Santos A unpublished
- [14] Acedo L and Santos A 1994 *Phys. Rev. E* **50** 4577